Supporting Information for

Crystal engineering, electron density analysis and in-situ variable temperature studies of co-crystal between nicotinic acid and gallic acid sesquihydrate.

Infal Iqbal[a], Arshad Mehmood,[b] Sajida Noureen*[a], Claude Lecomte[c,d], Maqsood Ahmed*[a]

[a]Materials Chemistry Laboratory, Institute of Chemistry, The Islamia University, of Bahawalpur, Baghdad-ul-Jadeed campus, 63100, Pakistan.

[b]Department of Chemistry & Biochemistry, Texas Christian University, Fort Worth, Texas, USA, 76129.

[c] Université de Lorraine; Laboratoire CRM2, UMR CNRS 7036, Boulevard des aiguillettes BP70239, Vandoeuvre-les-Nancy, 54506, France
[d] CNRS, Laboratoire CRM2, UMR CNRS 7036, Boulevard des aiguillettes BP70239, Vandoeure-les-Nancy, 54506, France.

Correspondence: sajida.noureen@iub.edu.pk, Maqsood.ahmed@iub.edu.pk

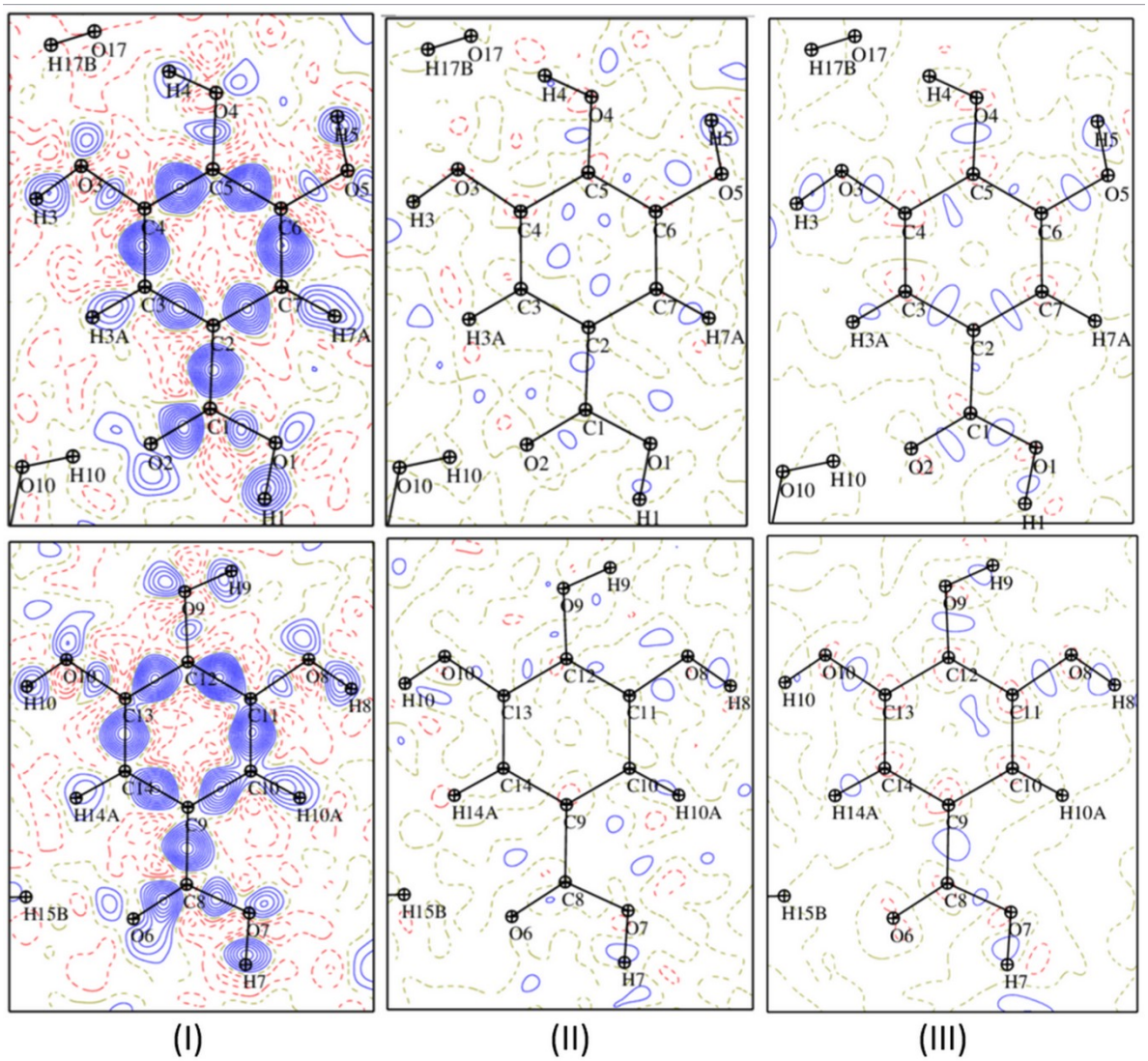

Figure S1A: Deformation electron density maps of GA1 and GA2 after IAM refinement (I), residual electron density maps after multipolar refinement experimental (II) and (III) after MM refinement of theoretical structure factors at contour level of 0.05 e Å^{-3} and with $\sin\theta_{Max}/\lambda$=0.7 Å^{-1}.

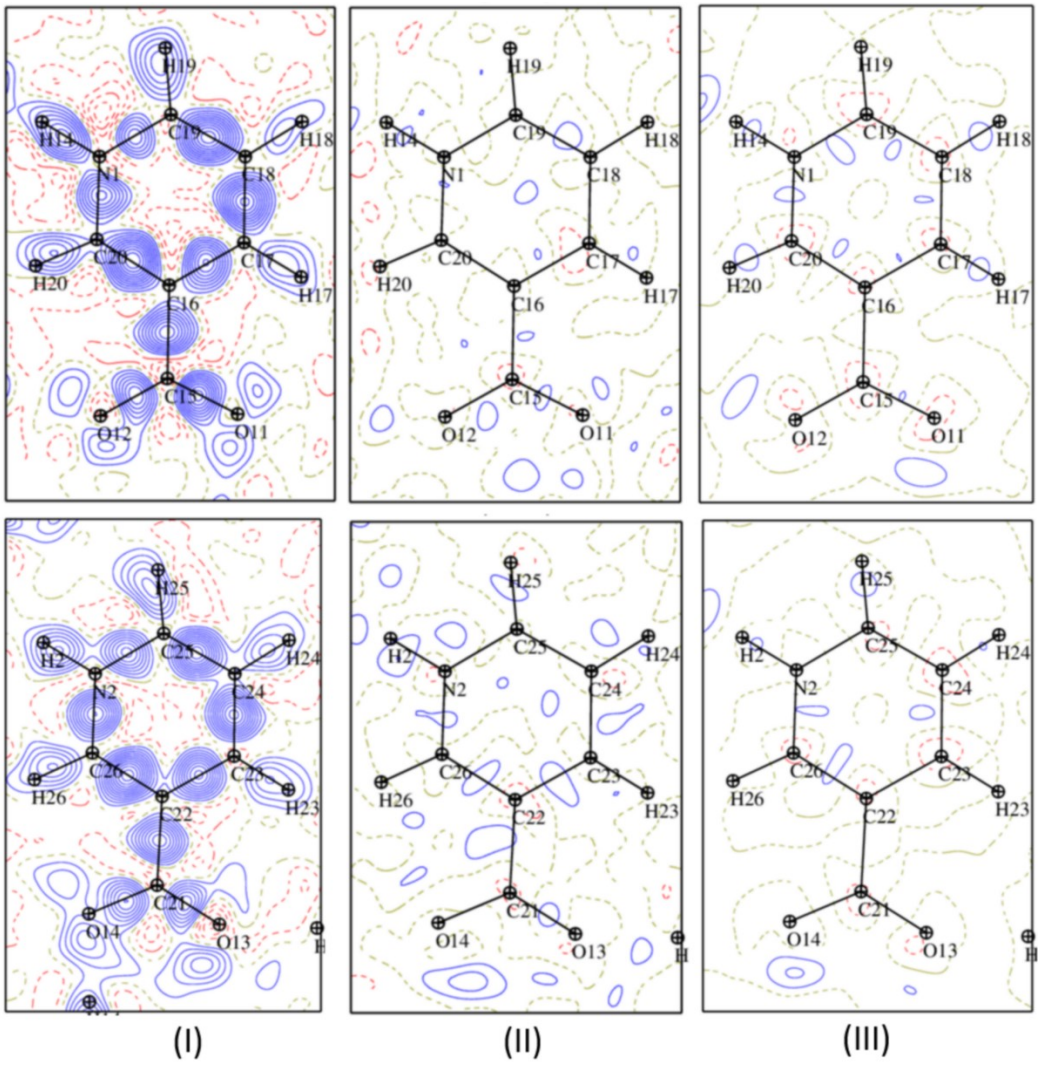

Figure S1B: Deformation electron density maps of NA1 and NA2 after IAM refinement (I), residual electron density maps after multipolar refinement experimental (II) and (III) after MM refinement of theoretical structure factors at contour level of 0.05 e $Å^{-3}$ and with $\sin\theta_{Max}/\lambda=0.7$ $Å^{-1}$.

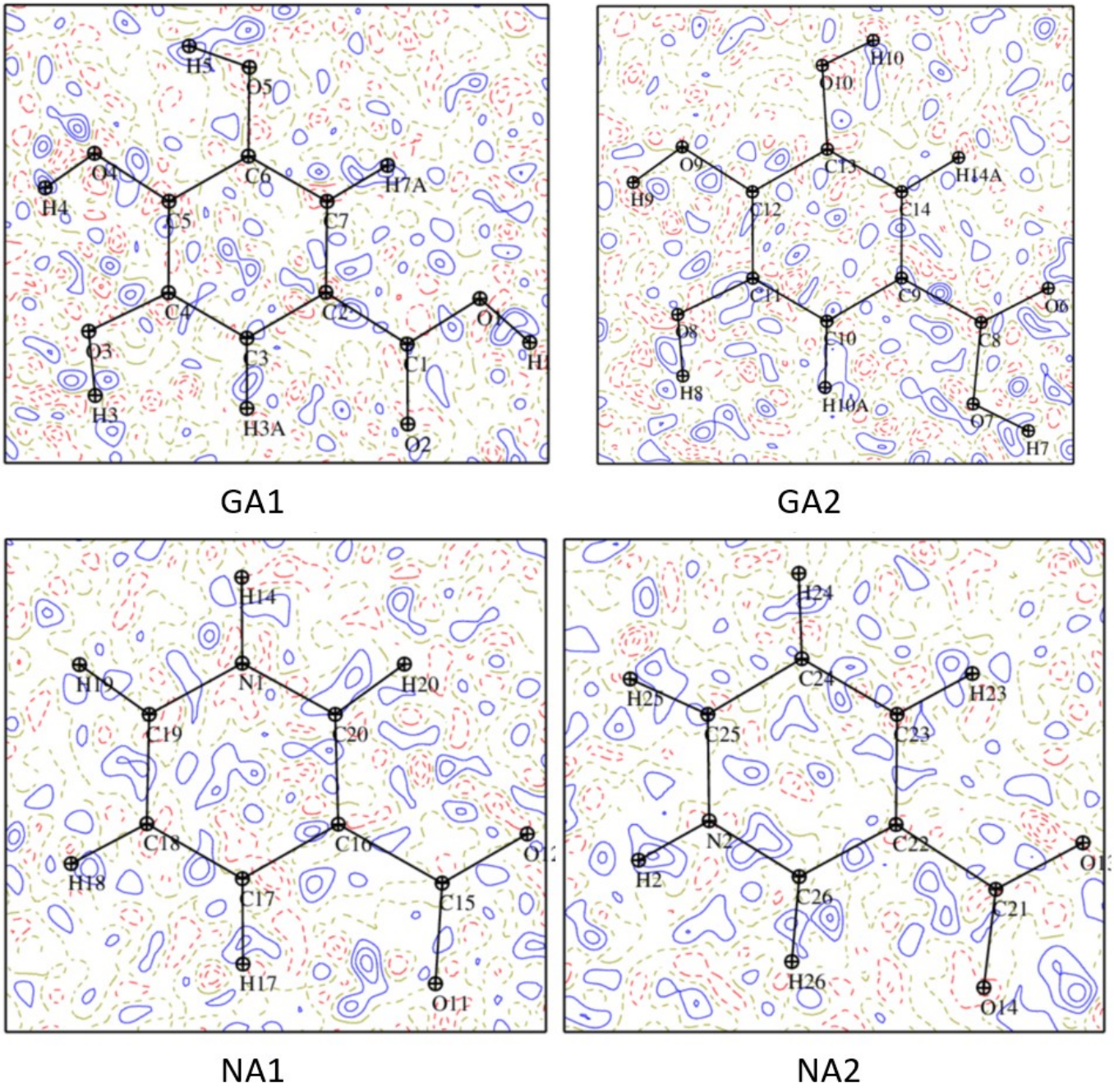

Figure 1SC: Residual electron density maps of GA1,GA2,NA1 and NA2 after experimentally multipolar refinement. contour level of 0.05 e Å^{-3} $\sin\theta_{Max}/\lambda$=1.163 Å^{-1}.

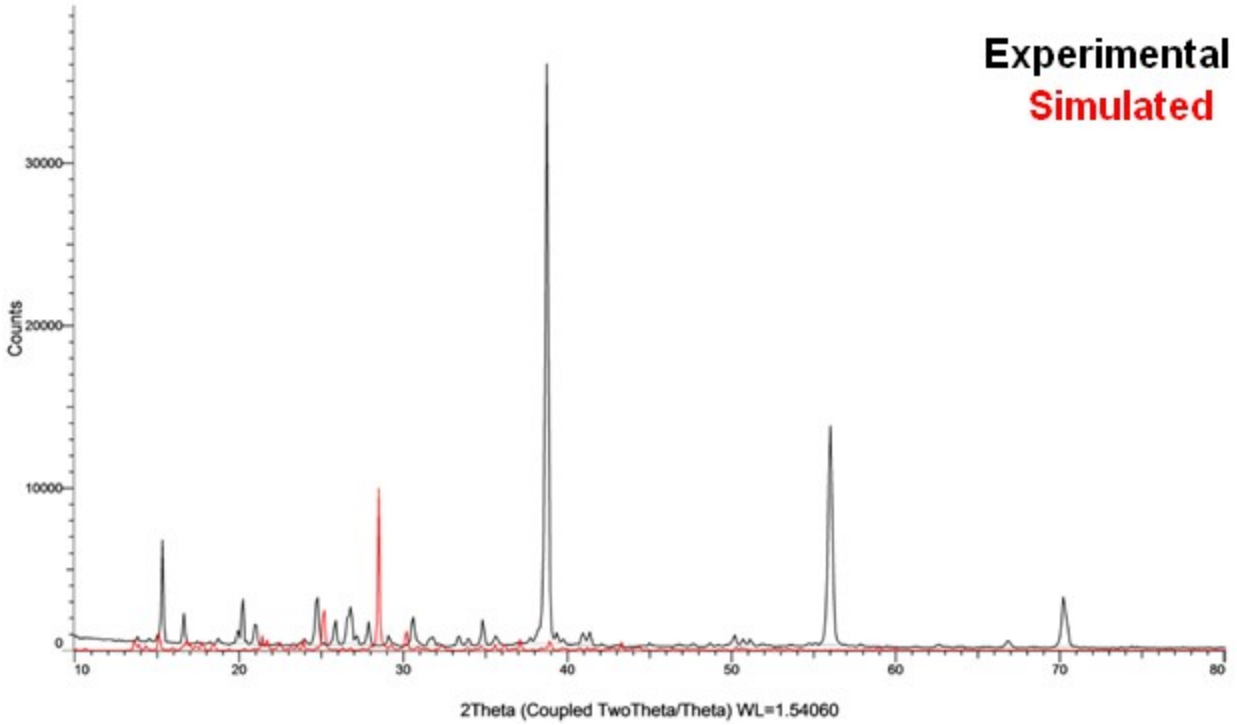

Figure S2(a): The powder XRD pattern of GANA co-crystal experimentally determined (black) and simulated powder pattern from single crystal data(red) using Mercury software. The intensity of the experimental pattern is manifold higher than the simulated. The position of the peaks till 50° is comparable, which is the upper limit of the simulated pattern.

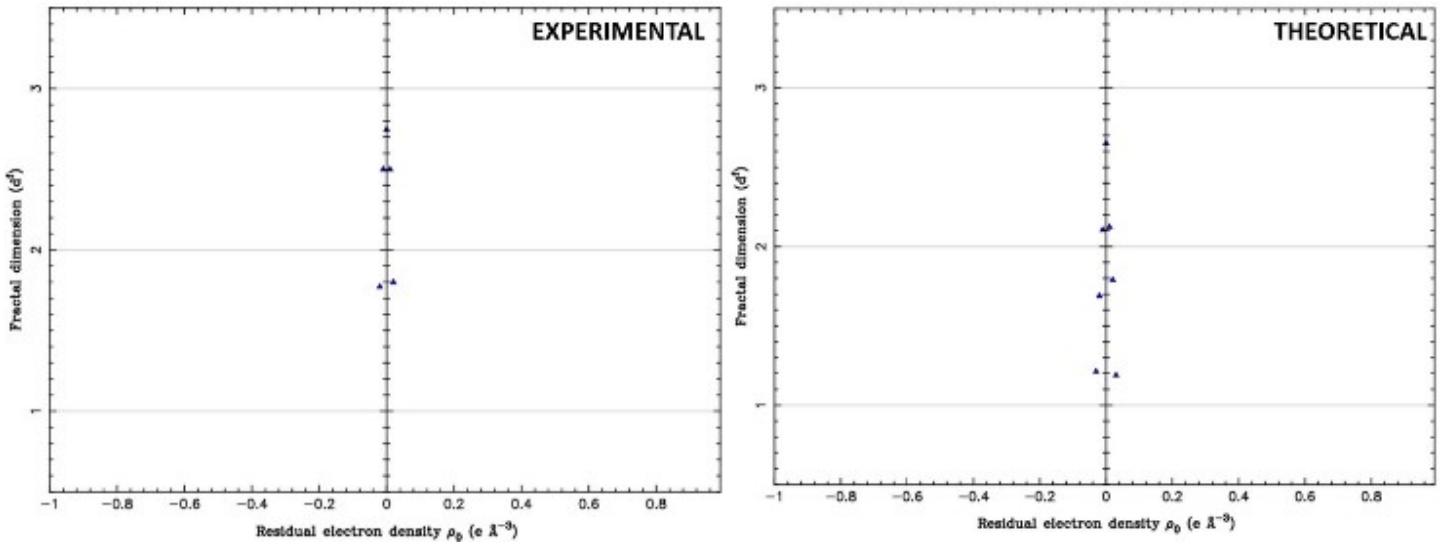

Figure S2(b): A fractal dimensions plot comparing the residual electron densities after experimental and theoretical (sinθ/λ of 1.163 Å-1) multipolar refinements.

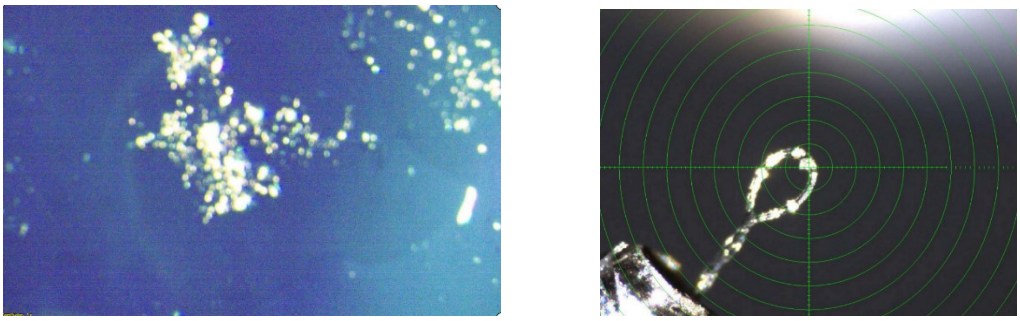

(a) *(b)*

Figure S3: Residual mass after in situ heating GANA co-crystal at 362K (*a)*, single crystal obtained from this residual mass (*b).*

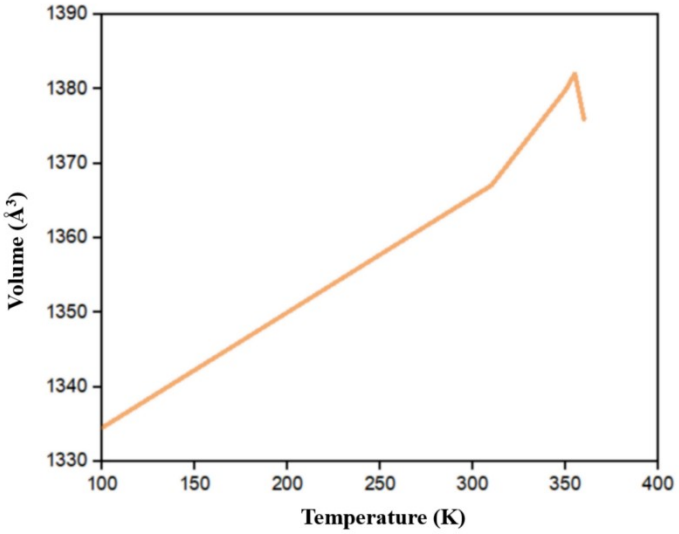

Figure S4: GANA co-crystal unit cell volume expansion with increase in temperature.

Table S1 (a): estimated ADPs for H atoms calculated from *SHADE* server.

Atom	U_{11}	U_{22}	U_{33}	U_{12}	U_{13}	U_{23}
H4	0.022712	0.025149	0.020224	0.0142	0.006122	0.001855
H14A	0.02818	0.03036	0.019821	0.019391	0.010529	0.001433
H19	0.028369	0.034685	0.013168	0.019246	0.005856	0.002328
H3A	0.028209	0.031886	0.023217	0.021452	0.011817	0.003951
H20	0.029919	0.032951	0.020766	0.022372	0.011424	0.003116
H7A	0.027088	0.03092	0.016197	0.017048	0.007241	0.001924
H25	0.025658	0.034985	0.019859	0.021885	0.005407	0.007092
H24	0.029928	0.030467	0.022195	0.021479	0.010366	0.003264
H18	0.031931	0.034269	0.021271	0.023485	0.012779	0.003657

H10A	0.023581	0.034819	0.021393	0.021696	0.00685	0.005508
H26	0.030384	0.029688	0.021138	0.020689	0.010438	0.002707
H23	0.026894	0.031858	0.013621	0.017524	0.004309	0.000875
H17	0.026802	0.037691	0.020796	0.024377	0.007548	0.007048
H15A	0.02248	0.029489	0.028434	0.011843	0.016221	0.008699
H15B	0.030115	0.019288	0.028899	0.014511	0.013689	0.007412
H17B	0.025787	0.03431	0.024794	0.018314	0.014452	0.008145
H17A	0.019581	0.034545	0.022786	0.016586	0.005392	0.00624
H16A	0.031352	0.026584	0.027024	0.018926	0.013291	0.012458
H16B	0.018047	0.029321	0.028417	0.010105	0.009768	0.005795
H7	0.021767	0.028612	0.013916	0.01508	0.004632	0.00188
H9	0.023543	0.028518	0.017479	0.017079	0.0089	0.003064
H10	0.022157	0.021741	0.019402	0.013125	0.006852	0.000637
H8	0.022628	0.029299	0.017859	0.018523	0.006741	0.005051
H14	0.026517	0.034037	0.018289	0.022358	0.006646	0.005722
H5	0.022635	0.028629	0.02088	0.017369	0.007871	0.006111
H1	0.021068	0.026421	0.019269	0.015984	0.007533	0.005112
H3	0.023231	0.029612	0.020839	0.018167	0.009677	0.004884
H2	0.028043	0.033191	0.013763	0.019091	0.005314	0.002199

Table S1 (b): Chemical equivalent constrains.

C14 C3 C7 C10
C12 C5
C11 C4 C13
C19 C25
C20 C26
C8 C1
C22 C16
C24 C18
C23 C17
H4 H9 H10 H8 H5 H3
H14A H3A H7A H10A
H19 H20 H25 H26
H24 H18
H23 H17
H15A H15B H17B H17A H16A H16B
H7 H1
H14 H2
H4 H15A H7
H14A H24 H23

Table S1(c): DFT calculated distances with restrain values.

Atom 1	Atom2	Distance (Å)	Restrain
O7	H7	0.99827	0.001
O1	H1	1.01827	0.001
O9	H9	0.99289	0.001
O10	H10	0.99878	0.001
O4	H4	0.99581	0.001
O5	H5	0.97843	0.001
O8	H8	1.00351	0.001
O3	H3	0.99675	0.001
N2	H2	1.02491	0.001
N1	H14	1.08752	0.001
O16	H16B	0.99508	0.001
O16	H16A	0.9953	0.001
O17	H17B	0.9819	0.001
O17	H17A	0.98564	0.001
O15	H15A	0.98713	0.001
O15	H15B	0.97777	0.001
C14	H14A	1.07852	0.001
C19	H19	1.08087	0.001
C3	H3A	1.07976	0.001
C20	H20	1.07945	0.001
C7	H7A	1.07977	0.001
C25	H25	1.07812	0.001
C24	H24	1.07882	0.001
C18	H18	1.08104	0.001
C10	H10A	1.07856	0.001
C26	H26	1.07993	0.001
C23	H23	1.082	0.001
C17	H17	1.07956	0.001

Table S2:

Effect of temperature on unit cell volume of co-crystal

	Temperature	Volume (Å^3)
1	100K	1334.57(6)
2	298K	1370.51 (9)
3	310K	1367.1(8)
4	350K	1379.9(15)
5	355K	1382.1(10)
6	360K	1376.0(11)
7	361K	33140(14) melting
8	365K	1406(5)

Table S3: Topological properties of (3, -1) CPs on the covalent interactions: distances (Å), electron density (eÅ^{-3}), Laplacian (eÅ^{-5}), Hessian eigenvalues (eÅ^{-5}), ε = ellipticity, G_{CP}= bond kinetic energy density (Hartree Å $^{-3}$) and V_{CP} = bond potential energy density (Hartree Å $^{-3}$).

The upper line in each pair gives the experimental values and the lower one the theoretical values.

	Interacting atoms	d_{12} (Å)	d1cp (Å)	d2cp (Å)	ρ(rb) (e/Å^3)	$\nabla^2\rho$(cp) (e/Å^5)	λ_1 (e/Å^5)	λ_2 (e/Å^5)	λ_3 (e/Å^5)	ε	Gcp	Vcp
1	O6—C8	1.226	0.809(2)	0.417(1)	2.828(3)	-23.832	-27.350	-24.620	28.140	0.111	3.435	-8.539
		1.226	0.775	0.451	2.704	-25.937	-23.05	-20.95	18.06	0.101	3.014	-7.913
2	O2—C1	1.230	0.811(1)	0.419(1)	2.814(2)	-25.223	-27.030	-24.340	26.160	0.111	3.332	-8.429
		1.230	0.769	0.461	2.654	-25.378	-22.550	-20.490	17.660	0.101	2.905	-7.587
3	O12—C15	1.245	0.824(2)	0.421(2)	2.671(1)	-21.401	-25.100	-23.170	26.870	0.083	3.135	-7.769
		1.245	0.768	0.477	2.602	-25.169	-21.910	-20.040	16.780	0.093	2.782	-7.326
4	O14—C21	1.260	0.825(1)	0.435(1)	2.638(3)	-29.727	-24.300	-22.310	16.880	0.089	2.661	-7.404
		1.260	0.772	0.488	2.544	-24.485	-20.800	-19.130	15.450	0.088	2.669	-7.052
5	O13—C21	1.257	0.820(2)	0.437(3)	2.630(3)	-30.433	-24.010	-22.380	15.960	0.073	2.610	-7.350
		1.257	0.773	0.484	2.515	-23.952	-20.480	-18.980	15.510	0.080	2.623	-6.922
6	O11—C15	1.278	0.835(1)	0.443(3)	2.552(1)	-29.998	-22.950	-21.510	14.460	0.067	2.431	-6.963

		1.278	0.770	0.508	2.402	-20.836	-19.530	-17.840	16.530	0.095	2.491	-6.442
7	N2—C26	1.339	0.822(1)	0.517(1)	2.360(3)	-29.120	-19.080	-16.850	6.810	0.133	2.005	-6.049
		1.339	0.773	0.566	2.166	-15.957	-17.120	-14.890	16.050	0.150	2.172	-5.461
8	N1—C20	1.341	0.811(1)	0.530(1)	2.337(2)	-27.854	-18.750	-16.660	7.560	0.126	2.010	-5.970
		1.341	0.766	0.575	2.149	-14.724	-16.740	-14.770	16.790	0.134	2.191	-5.412
9	N2—C25	1.346	0.818(1)	0.527(1)	2.302(1)	-25.607	-17.850	-15.920	8.160	0.121	2.032	-5.857
		1.346	0.786	0.560	2.148	-16.331	-16.510	-14.930	15.100	0.106	2.112	-5.367
10	N1—C19	1.342	0.811(1)	0.531(1)	2.294(3)	-25.244	-17.670	-15.940	8.370	0.109	2.029	-5.826
		1.342	0.771	0.571	2.162	-15.201	-16.710	-14.690	16.200	0.137	2.196	-5.456
11	C25—C24	1.382	0.707(1)	0.675(1)	2.233(1)	-21.805	-17.030	-14.050	9.280	0.212	2.049	-5.625
		1.382	0.712	0.670	2.103	-15.982	-16.090	-13.620	13.730	0.181	2.028	-5.176
12	C19—C18	1.384	0.708(1)	0.676(1)	2.227(2)	-21.640	-16.970	-14.000	9.330	0.212	2.044	-5.603
		1.384	0.710	0.674	2.094	-15.695	-16.030	-13.450	13.780	0.191	2.024	-5.147
13	O1—C1	1.319	0.866(1)	0.453(1)	2.225(1)	-24.501	-18.380	-17.750	11.630	0.036	1.906	-5.528
		1.319	0.794	0.525	2.129	-16.222	-16.560	-15.600	15.940	0.062	2.076	-5.287
14	O7—C8	1.329	0.873(2)	0.457(1)	2.220(2)	-25.047	-18.330	-17.550	10.830	0.045	1.868	-5.490
		1.329	0.793	0.537	2.114	-15.408	-16.410	-15.410	16.420	0.065	2.08	-5.239
15	C20—C16	1.388	0.725(1)	0.663(2)	2.214(1)	-21.162	-17.010	-13.980	9.820	0.216	2.036	-5.553
		1.388	0.713	0.676	2.085	-15.620	-15.920	-13.350	13.640	0.193	2.008	-5.11
16	C22—C26	1.390	0.664(1)	0.726(1)	2.207(1)	-21.008	-16.950	-13.930	9.880	0.217	2.028	-5.528
		1.390	0.678	0.712	2.046	-	-	-13.030	13.450	0.206	1.938	-4.946

						15.294	15.710					
17	C3—C4	1.389	0.679(2)	0.710(1)	2.194(1)	-20.729	-17.160	-13.400	9.830	0.281	2.011	-5.473
		1.389	0.684	0.706	2.070	-15.277	-15.920	-12.900	13.540	0.234	1.991	-5.051
18	C14—C13	1.392	0.681(1)	0.710(1)	2.189(1)	-20.546	-17.110	-13.350	9.920	0.282	2.008	-5.454
		1.392	0.678	0.714	2.050	-14.873	-15.870	-12.520	13.520	0.268	1.966	-4.973
19	C11—C10	1.392	0.711(1)	0.681(1)	2.189(1)	-20.540	-17.110	-13.350	9.920	0.281	2.008	-5.455
		1.392	0.720	0.671	2.064	-15.205	-16.100	-12.570	13.460	0.281	1.981	-5.026
20	C18—C17	1.392	0.681(1)	0.711(1)	2.184(1)	-20.942	-16.650	-13.970	9.680	0.192	1.978	-5.423
		1.392	0.691	0.701	2.018	-14.706	-15.250	-13.120	13.670	0.163	1.904	-4.838
21	C24—C23	1.395	0.682(1)	0.713(1)	2.176(1)	-20.738	-16.580	-13.900	9.750	0.192	1.970	-5.392
		1.395	0.691	0.704	2.042	-14.709	-15.350	-13.270	13.910	0.157	1.955	-4.94
22	O15—H15B	0.977	0.769(1)	0.208(1)	2.175(2)	-36.993	-34.380	-34.290	31.680	0.002	1.209	-5.007
		0.977	0.732	0.245	2.225	-24.971	-30.750	-30.590	36.370	0.005	1.883	-5.514
23	O5—H5	0.979	0.764(1)	0.215(1)	2.173(1)	-34.706	-34.550	-34.410	34.260	0.004	1.311	-5.053
		0.979	0.739	0.240	2.143	-25.181	-30.440	-30.270	35.520	0.006	1.688	-5.138
24	C6—C5	1.400	0.708(2)	0.692(1)	2.165(1)	-20.398	-17.460	-13.200	10.260	0.323	1.962	-5.353
		1.400	0.698	0.703	2.026	-15.571	-16.060	-12.440	12.930	0.290	1.882	-4.853
25	C12—C13	1.398	0.702(1)	0.697(1)	2.164(1)	-20.546	-17.360	-13.010	9.820	0.334	1.953	-5.344
		1.398	0.699	0.700	2.118	-16.748	-16.900	-13.030	13.190	0.297	2.026	-5.224
26	C12—C11	1.403	0.704(2)	0.699(1)	2.156(1)	-20.317	-17.150	-13.060	9.890	0.313	1.945	-5.313
		1.403	0.709	0.694	2.067	-15.906	-16.500	-12.550	13.140	0.314	1.955	-5.023

28	C4—C5	1.403	0.700(1)	0.704	2.154	-20.303	-17.130	-13.050	9.880	0.313	1.941	-5.304
		1.403	0.707	0.697	2.035	-15.346	-16.060	-12.420	13.130	0.293	1.910	-4.895
29	C6—C7	1.391	0.709	0.683	2.152	-20.134	-16.910	-13.340	10.120	0.268	1.944	-5.297
		1.391	0.713	0.678	2.068	-15.403	-16.050	-12.800	13.450	0.254	1.979	-5.036
30	C22—C23	1.393	0.678	0.716	2.147	-19.866	-16.250	-13.690	10.080	0.187	1.946	-5.284
		1.393	0.689	0.705	2.066	-15.734	-15.700	-13.360	13.330	0.175	1.960	-5.021
31	C16—C17	1.395	0.679	0.716	2.142	-19.742	-16.210	-13.650	10.120	0.187	1.941	-5.265
		1.395	0.697	0.697	2.023	-14.976	-15.230	-13.010	13.260	0.171	1.903	-4.855
32	O17—H17B	0.982	0.769	0.213	2.140	-34.915	-33.360	-33.030	31.480	0.010	1.228	-4.901
		0.982	0.741	0.241	2.145	-24.905	-30.140	-29.900	35.140	0.008	1.707	-5.157
33	O9—H9	0.992	0.772	0.221	2.139	-32.541	-33.440	-32.970	33.860	0.014	1.336	-4.950
		0.992	0.752	0.241	2.043	-23.050	-28.950	-28.710	34.610	0.008	1.569	-4.752
34	O16—H16B	0.995	0.779	0.216	2.136	-34.582	-32.990	-32.550	30.960	0.013	1.234	-4.890
		0.995	0.751	0.244	2.055	-22.606	-28.480	-28.210	34.090	0.009	1.616	-4.815
35	O16—H16A	0.995	0.779(2)	0.216(2)	2.136(1)	-34.580	-32.980	-32.550	30.960	0.013	1.235	-4.890
		0.995	0.748	0.247	2.059	-21.025	-28.110	-27.880	34.960	0.008	1.698	-4.869
36	O15—H15A	0.987	0.773(2)	0.214(2)	2.135(2)	-34.502	-32.980	-32.830	31.310	0.005	1.235	-4.886
		0.987	0.744	0.242	2.127	-24.453	-29.740	-29.520	34.810	0.007	1.688	-5.087
37	O17—H17A	0.985	0.770(1)	0.214(1)	2.128(1)	-34.169	-32.940	-32.600	31.370	0.010	1.236	-4.863
		0.985	0.746	0.239	2.099	-24.303	-29.650	-29.360	34.700	0.010	1.632	-4.965
38	O3—H3	0.996	0.773(1)	0.224(2)	2.121(2)	-	-	-32.190	33.780	0.016	1.361	-4.902

						31.130	32.720					
		0.996	0.754	0.243	1.998	-20.110	-27.770	-27.550	35.210	0.008	1.609	-4.626
38	O4—H4	0.995	0.771(1)	0.224(2)	2.116(1)	-31.006	-32.500	-32.220	33.710	0.009	1.357	-4.885
		0.995	0.754	0.241	2.041	-23.419	-28.820	-28.760	34.170	0.002	1.547	-4.733
39	O10—H10	0.998	0.771(2)	0.227(1)	2.102(1)	-29.966	-32.140	-31.410	33.580	0.023	1.375	-4.849
		0.998	0.754	0.244	2.037	-22.972	-28.650	-28.240	33.920	0.015	1.559	-4.727
40	O8—H8	1.003	0.776(1)	0.227(2)	2.101(3)	-29.892	-31.940	-31.640	33.690	0.009	1.376	-4.845
		1.003	0.761	0.242	1.979	-21.636	-27.760	-27.670	33.790	0.003	1.498	-4.510
41	C9—C14	1.400	0.698(1)	0.702(2)	2.095(2)	-18.477	-15.970	-12.740	10.230	0.253	1.896	-5.085
		1.400	0.706	0.694	1.989	-13.729	-14.900	-12.130	13.300	0.228	1.889	-4.740
42	C9—C10	1.401	0.698(1)	0.703(1)	2.090(2)	-18.444	-15.970	-12.720	10.240	0.256	1.887	-5.065
		1.401	0.697	0.704	1.979	-13.900	-14.920	-12.270	13.280	0.216	1.860	-4.693
43	C2—C7	1.398	0.705(1)	0.694(2)	2.088(2)	-18.444	-15.930	-12.950	10.430	0.230	1.882	-5.055
		1.398	0.699	0.700	1.969	-13.395	-14.820	-12.240	13.660	0.211	1.861	-4.660
44	C2—C3	1.400	0.701(1)	0.699(1)	2.068(3)	-17.991	-15.790	-12.670	10.470	0.247	1.860	-4.980
		1.400	0.701	0.698	1.936	-12.900	-14.560	-11.930	13.590	0.220	1.815	-4.533
45	O8—C11	1.353	0.826(1)	0.528(2)	2.068(1)	-19.563	-16.160	-14.740	11.340	0.096	1.786	-4.941
		1.353	0.793	0.560	1.946	-10.102	-14.400	-13.670	17.970	0.054	1.968	-4.643
46	O9—C12	1.355	0.828(1)	0.527(1)	2.050(2)	-18.363	-15.990	-14.410	12.040	0.110	1.803	-4.891
		1.355	0.792	0.563	1.922	-9.198	-14.500	-13.160	18.460	0.102	1.961	-4.565
47	O3—C4	1.359	0.822(1)	0.537(1)	2.049(2)	-18.787	-16.070	-14.510	11.790	0.107	1.781	-4.877

		1.359	0.792	0.567	1.915	-8.731	-13.950	-13.210	18.420	0.056	1.966	-4.543
48	O10—C13	1.366	0.826(1)	0.540(1)	2.041(2)	-18.423	-15.970	-14.460	12.010	0.105	1.781	-4.851
		1.366	0.795	0.571	1.872	-7.998	-13.640	-12.760	18.400	0.069	1.913	-4.386
49	O4—C5	1.360	0.829(1)	0.531(1)	2.036(1)	-17.911	-15.790	-14.350	12.230	0.100	1.794	-4.841
		1.360	0.792	0.567	1.912	-8.226	-14.060	-12.910	18.740	0.089	1.984	-4.544
50	O7—H7	0.997	0.780(1)	0.218(2)	2.028(2)	-29.831	-31.230	-31.120	32.520	0.004	1.221	-4.530
		0.997	0.759	0.238	2.008	-22.351	-27.820	-27.670	33.140	0.005	1.527	-4.620
51	O1—H1	1.018	0.790(2)	0.227(1)	1.971(3)	-26.031	-29.110	-29.100	32.180	0.001	1.275	-4.373
		1.018	0.771	0.247	1.924	-20.244	-25.910	-25.900	31.570	0.001	1.449	-4.316
52	O5—C6	1.366	0.836(1)	0.531(2)	1.965(1)	-17.719	-15.220	-14.030	11.540	0.085	1.652	-4.544
		1.366	0.796	0.571	1.871	-7.852	-13.910	-12.600	18.660	0.104	1.917	-4.384
53	C2—C1	1.479	0.696(1)	0.783(1)	1.883(1)	-16.707	-14.220	-11.670	9.180	0.218	1.528	-4.226
		1.479	0.701	0.777	1.769	-11.418	-12.940	-11.020	12.540	0.174	1.547	-3.893
54	C26—H26	1.079	0.741(1)	0.338(1)	1.865(2)	-18.836	-18.810	-17.730	17.700	0.060	1.392	-4.103
		1.079	0.721	0.358	1.918	-18.157	-18.780	-18.130	18.760	0.036	1.534	-4.339
55	C20—H20	1.079	0.742(1)	0.338(2)	1.864(1)	-18.784	-18.770	-17.730	17.720	0.059	1.393	-4.101
		1.079	0.723	0.357	1.875	-17.042	-18.260	-17.630	18.840	0.036	1.496	-4.185
56	C9—C8	1.483	0.689(1)	0.794(1)	1.856(3)	-16.125	-13.970	-11.290	9.140	0.238	1.501	-4.132
		1.483	0.708	0.775	1.709	-10.965	-12.670	-10.670	12.370	0.188	1.453	-3.673
57	C17—H17	1.079	0.735(1)	0.344(1)	1.839(3)	-18.356	-18.130	-17.330	17.110	0.046	1.362	-4.009
		1.079	0.721	0.358	1.852	-	-	-17.400	18.410	0.014	1.470	-4.103

						16.619	17.630					
58	N2—H2	1.025	0.796(2)	0.229(1)	1.836(1)	-19.941	-25.250	-25.200	30.510	0.002	1.282	-3.960
		1.025	0.775	0.250	1.998	-21.846	-26.220	-25.650	30.020	0.022	1.529	-4.587
59	C25—H25	1.078	0.733(1)	0.345(1)	1.836(1)	-17.964	-18.010	-17.110	17.150	0.053	1.374	-4.006
		1.078	0.720	0.358	1.869	-16.928	-17.950	-17.520	18.550	0.024	1.489	-4.163
60	C10—H10A	1.078	0.716(1)	0.362(1)	1.832(3)	-17.088	-17.540	-16.560	17.010	0.059	1.408	-4.011
		1.078	0.704	0.374	1.841	-15.674	-17.250	-16.460	18.040	0.048	1.492	-4.082
61	C14—H14A	1.078	0.717(2)	0.362(1)	1.831(2)	-17.074	-17.540	-16.550	17.010	0.060	1.407	-4.009
		1.078	0.706	0.373	1.797	-14.995	-16.790	-16.100	17.900	0.043	1.436	-3.922
62	C23—H23	1.082	0.737(1)	0.345(2)	1.830(1)	-18.136	-17.960	-17.270	17.090	0.040	1.355	-3.979
		1.082	0.717	0.365	1.867	-16.447	-17.540	-17.380	18.470	0.010	1.508	-4.167
63	C19—H19	1.081	0.736(1)	0.346(2)	1.827(1)	-17.741	-17.860	-17.010	17.130	0.050	1.366	-3.975
		1.081	0.725	0.356	1.893	-16.897	-18.100	-17.760	18.970	0.019	1.541	-4.265
64	C3—H3A	1.079	0.717(1)	0.363(1)	1.826(2)	-16.997	-17.480	-16.490	16.970	0.060	1.400	-3.991
		1.079	0.701	0.379	1.801	-15.072	-16.710	-15.900	17.540	0.051	1.439	-3.934
65	C7—H7A	1.080	0.717(1)	0.363(2)	1.824(1)	-16.980	-17.440	-16.470	16.930	0.059	1.397	-3.982
		1.080	0.706	0.374	1.824	-15.343	-16.980	-16.380	18.020	0.037	1.473	-4.021
66	C24—H24	1.079	0.741(1)	0.337(1)	1.802(3)	-17.977	-17.760	-17.060	16.840	0.041	1.306	-3.870
		1.079	0.712	0.366	1.847	-16.011	-17.250	-16.850	18.090	0.024	1.489	-4.098
67	C18—H18	1.081	0.743(1)	0.338(1)	1.796(1)	-17.841	-17.680	-16.980	16.820	0.041	1.301	-3.851
		1.081	0.715	0.366	1.838	-16.129	-17.280	-16.780	17.940	0.030	1.464	-4.058

68	C22—C21	1.504	0.736(1)	0.769(2)	1.781(2)	-14.051	-13.050	-11.100	10.100	0.175	1.448	-3.880
		1.504	0.750	0.754	1.702	-10.527	-12.360	-10.820	12.660	0.143	1.460	-3.658
69	C15—C16	1.509	0.761(1)	0.748(1)	1.740(3)	-13.665	-12.550	-11.010	9.900	0.140	1.386	-3.729
		1.509	0.761	0.748	1.684	-10.053	-12.200	-10.700	12.860	0.140	1.447	-3.597
70	N1—H14	1.087	0.829(1)	0.258(1)	1.628(3)	-12.432	-20.450	-19.860	27.870	0.030	1.231	-3.332
		1.087	0.821	0.267	1.671	-13.118	-20.280	-19.970	27.130	0.015	1.280	-3.478

Hirshfeld Surface Analysis and Fingerprint plots

The Hirshfeld surface alongwith interacting neighboring molecules is shown in figure S7, red spots in the vicinity of all oxygen and nitrogen atoms highlight the stronger intermolecular interactions while white region shows the weak H···H contacts. Fingerprint plots of co-crystal (Figure S8) were generated with d_{norm}, normalized contact distance in terms of d_e and d_i, using *CrystalExplorer* [45]. The two sharp spikes exhibiting the O···H/H···O contacts accounting 37.9% of interactions, the broader region between these spikes shows the H···H contacts of 26.54% of total interactions indicates that these short contacts play a crucial role in the co-crystal assembly, while the wing shaped upper area shows the H···C/C···H interactions of 16.1%. Moreover, O···C, C···C, N···H and O···O interactions show 10.2%, 5.5%, 1.4%and 1.3% contribution in co-crystal assembly and its packing; whereas the N···C interactions contribute relatively less with corresponding value of 0.5%. This analysis depicts that O···H interactions are the major contributing interactions involved in co-crystal assembly and crystal water molecules are responsible for these interactions.

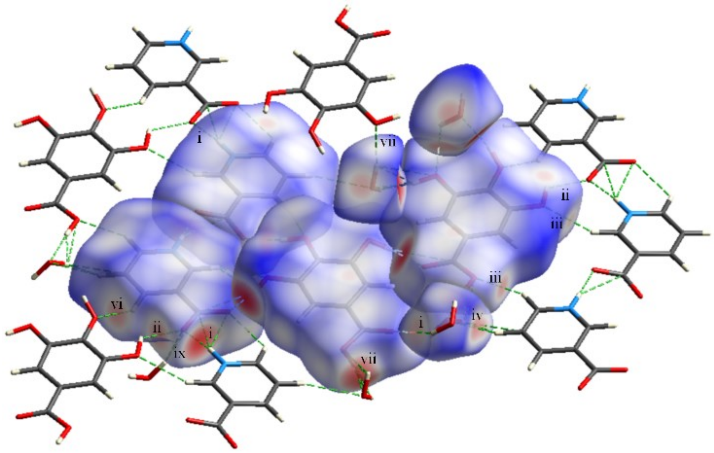

Figure S5: The Hirshfeld surface of GANA co-crystal, with its interacting molecules. The symmetry codes are same as in table 2.

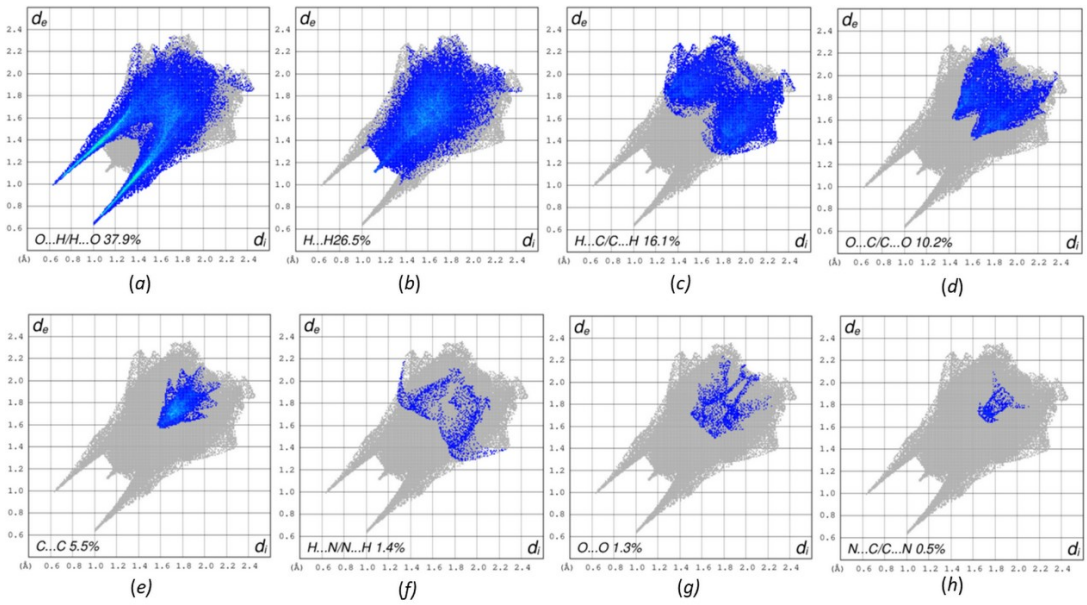

Figure S6: Fingerprint plots showing the percentage of interactions in the GANA co-crystal.

Electron density maps and topological study of covalent bonds

The static deformation density maps of all the molecules after experimental and theoretical multipole refinement (figure S9) show the accumulation of electron density between the connected atoms, nature of bonding and oxygen atoms lone pairs position of carbonyl and hydroxyl groups of all molecules. All the carbonyl oxygen atoms O2, O6, O12, O13 and carboxylate (O11 and O14) lone pairs are bilobed, while the lone pair of water molecules are in tetrahedral manner above and below the plane of water molecule as shown in figure S10 for O17-water molecule. All these findings are consistent with the detailed analysis of lone pairs of oxygen acceptor atom of carbonyl and hydroxyl groups in literature [51] and both experimental and theoretical static electron density maps are in agreement. For comprehensive analysis of intramolecular and intermolecular interactions involved in co-crystal assembly, the topological analysis of the electron density of co-crystal based on QTAIM [34] has been performed using *VMoPro* [52]. The bond critical points (*bcps*) search for all bonds found (3, -1) and negative value of Laplacian of electron density, which reflects the covalent bond nature of all bonds in the co-crystal. In homonuclear C—C bonds, the *bcps* are present in the middle, while in hetronuclear bonds (O—C, N—C, C—H, N—H, O—H) the *bcps* are away from the middle of the bond and shifted towards the either electropositive atom. The experimental topological properties including electron density ρ_{bcp} (r) and the Laplacian of electron density $\nabla^2\rho_{bcp}$ (r) of cocrystal have been calculated and compared with the corresponding theoretical structure factors from DFT calculations in the cocrystal (Table S1).

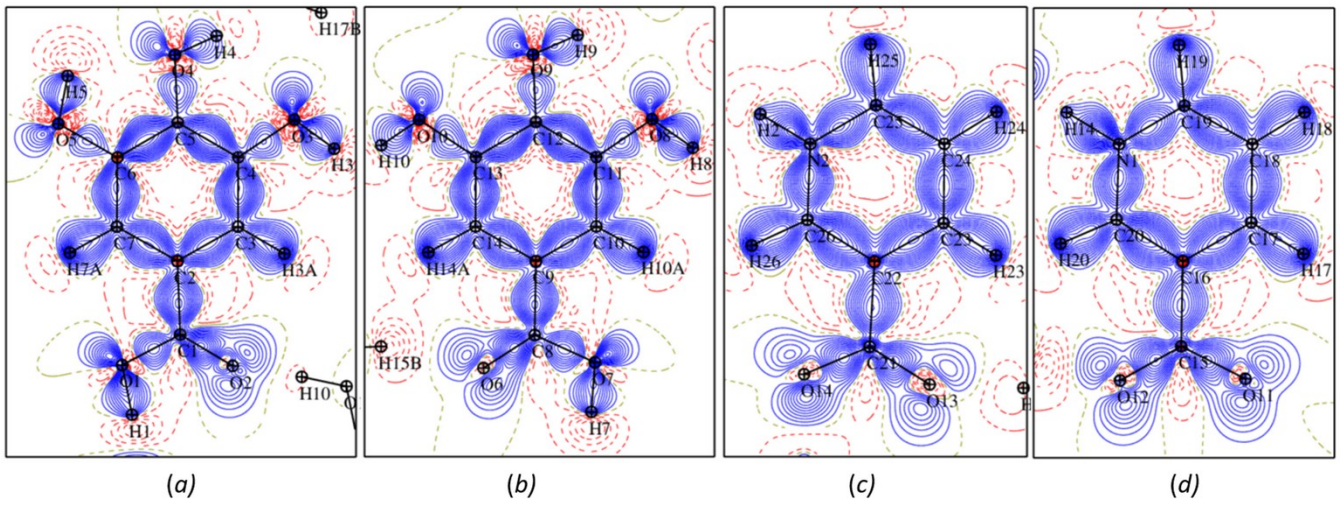

Figure S7(*a*): The static electron density maps of experimental data (a) GA1 molecule, (b) GA2 molecule, (c) NA1 molecule and (d) NA2 molecule.

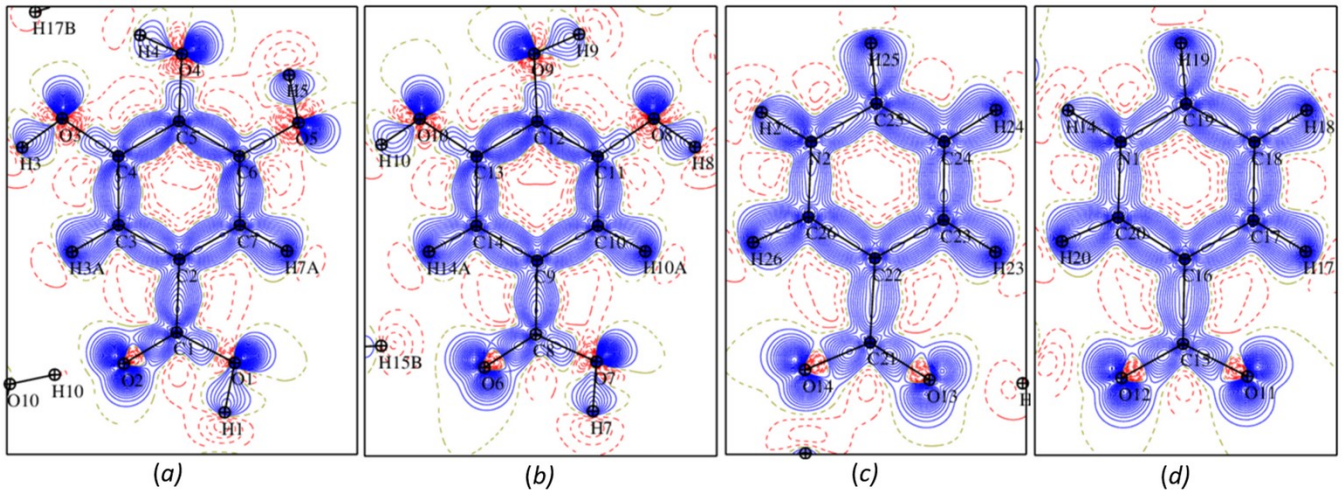

Figure S7(*b*): The static electron density maps of Theoretical data (a) GA1 molecule, (b) GA2 molecule, (c) NA1 molecule and (d) NA2 molecule.

Electron density ρ_{bcp} (r):

Electron density, a physical observable quantity which is maximum around nuclei and appears to be featureless away from nuclei. It is used to describe the bonding situation and chemical reactivity [53].The electron density ρ_{cp} (r) in the aromatic ring C—C bond ranges from 1.96/1.87eÅ^{-3} to 2.23/2.10 eÅ^{-3} in which C24—C25 bonding region of NA2 molecule has highest charge accumulation, the corresponding

experimental and theoretical electron density ρ_{cp} (r) values are 2.23 eÅ^{-3} and 2.10 eÅ^{-3} respectively. As expected, all non-aromatic C—C bonds have low charge accumulation as compared to aromatic bonds following the same trend in the theory with the corresponding average value of electron density 1.82 eÅ^{-3} and 1.72 eÅ^{-3} respectively. The C=O bond of carboxyl groups of GA molecules have highest charge accumulation at the *bcp*$_s$, with corresponding average values of experimental and theoretical electron density 2.82eÅ^{-3} and 2.68 eÅ^{-3} respectively. In NA molecules, the carboxylate anion (C=O$^-$) and C=O bonds have almost equal charge accumulation with an average value of 2.62 eÅ^{-3} and 2.52 eÅ^{-3} for experimental and theoretical electron densities respectively. [Table S3]. The C—H bonds of aromatic rings of GA and NA molecules have almost equal charge accumulation with an average electron density value 1.83/1.85 eÅ^{-3}. Among O—H bonds, the charge accumulation in carboxyl group and aromatic hydroxyl groups is unequal; the charges in the O—H aromatic ring bonds is highly concentrated [average value 2.12/2.04eÅ^{-3}] as compared to O—H carboxyl bond [1.99/1.97eÅ^{-3}]. Relatively, the average electron density of O—H bonds of water molecules is 2.14 eÅ^{-3} and 2.12 eÅ^{-3} for experimental and theoretical respectively. In C—N$^+$—H bonds of pyridinum zwitterion, C—N bonds have an average charge accumulation of 2.33/2.16 eÅ^{-3}, while N—H bonds have an average electron density of 1.73/1.83 eÅ^{-3}, in N—H bond the predicted electron density value is greater than the experimentally determined electron density.

Laplacian of electron density $\nabla^2\rho$bcp(r):

Laplaican of electron density, an important electronic property at *bcps*, explains the nature of bonds in a molecule. Topological analysis including Laplacian of electron density$\nabla^2\rho_{bcp}$ (r) has been carried out for experimental and theoretical structure factors and their comparison is given in table S3 and figure S11. In this GANA co-crystal, the Laplacian of electron density $\nabla^2\rho_{bcp}$ (r) at all the *bcps* is negative, so the electronic charge is locally concentrated and potential energy dominates, which exhibits the shared shell interactions termed as covalent bonds. The relief maps of the Laplacian of electron density in aromatic ring planes of experimental data and these maps are in good agreement with the theoretical maps in figure S8. In the aromatic C—C bonds of co-crystal, the Laplacian of electron density $\nabla^2\rho_{bcp}$ (r) ranges from -17.72/-7.85 eÅ^{-5} to -21.80/-15.98 eÅ^{-5}, while the Laplacian of electron density of non-aromatic C—C bond ranges from -13.66/-10.05 eÅ^{-5} to -16.70/-11.42 eÅ^{-5}. Among all aromatic C—C bonds, the Laplacian of electron density $\nabla^2\rho_{bcp}$ (r) of C24—C25 is highest, -21.80/-15.98 eÅ^{-5} that shows the charges at this bond are highly concentrated. In co-crystal, the carbonyl group C=O have relatively high value of Laplacian of electron density $\nabla^2\rho_{bcp}$ (r) as compared to all other bonds, this high value depicts the accumulation of charge in the

carbonyl bond. The Laplacian of electron density $\nabla^2\rho_{bcp}$ (r) of carbonyl bonds C=O bonds of both NA molecules (1 and 2) are quite different [C15=O12: -21.40/-25.16eÅ^{-5}; C21=O13: -30.43/25.17eÅ^{-5}].

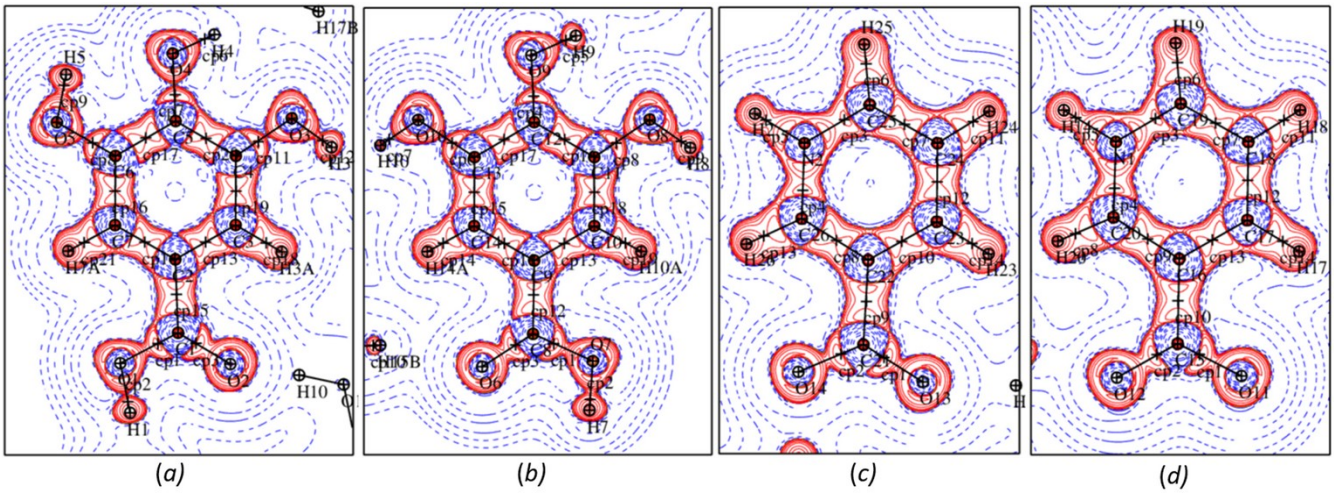

Figure S8 (*a*): The relief maps of Laplacian of electron density using experimental structure factors data (a) GA1 molecule, (b) GA2 molecule, (c) NA1 molecule and (d) NA2 molecule.

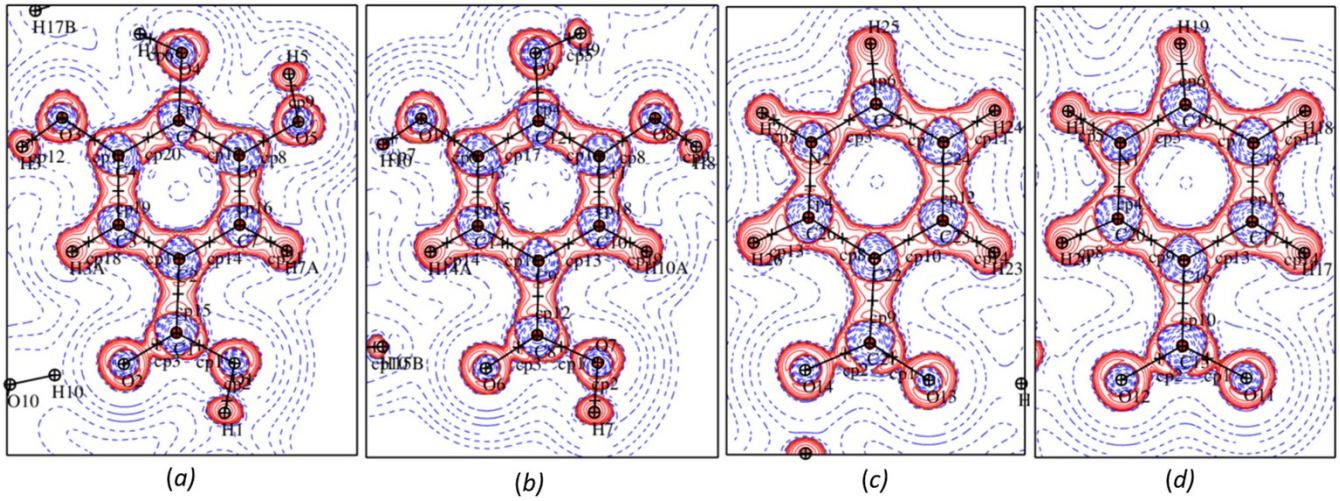

Figure S8 (*b*): The relief maps of Laplacian of electron density using theoretical structure factors (a) GA1 molecule, (b) GA2 molecule, (c) NA1 molecule and (d) NA2 molecule.

Table S4: Topological properties of (3, -1) CPs on the intermolecular interactions: distances (Å), electron density (eÅ^{-3}), Laplacian (eÅ^{-5}), Hessian eigenvalues (eÅ^{-5}), ε = ellipticity, Gcp = Bond Kinetic energy Vcp= Bond Potential Energy (Haretee/Å^3). The upper line in each pair gives the experimental values and the lower one the theoretical values.

	Interactions	Interacting species	d_{12} (Å)	$d1$cp (Å)	$d2$cp (Å)	ρ(rb) (e/Å^3)	$\nabla^2\rho$(cp) (e/Å^5)	Gcp (Hartree/Å^3)	Vcp (Hartree/Å^3)	ε
1	C19—H19···O1^{iii}	NA1···GA1	2.341(1)	0.957(2)	1.405(1)	0.058(2)	1.040(2)	0.054	-0.034	0.015
			2.341	0.973	1.380	0.072(1)	1.115	0.054	-0.040	0.003
2	C26···O2	NA2···GA1	3.049(1)	1.610(1)	1.463(2)	0.057(1)	0.742(3)	0.040	-0.027	0.243
			3.049	1.627	1.461	0.051	0.730	0.040	-0.027	0.411
3	C12···C24	GA2···NA2	3.192(1)	1.641(2)	1.583(1)	0.056(2)	0.586(1)	0.034	-0.020	0.920
			3.192	1.639	1.568	0.048	0.571	0.034	-0.020	1.131
4	O17—H17A···O9	O17water···GA2	2.367(1)	0.942(2)	1.460(2)	0.053(3)	0.929(1)	0.047	-0.027	0.135
			2.367	0.954	1.421	0.059	0.933	0.047	-0.034	0.059
5	C25···O5	NA2···GA1	3.085(1)	1.542(1)	1.546(1)	0.047(1)	0.657(3)	0.034	-0.020	0.637
			3.085	1.546	1.545	0.044	0.629	0.034	-0.020	0.567
6	C26—H26···O5^{iii}	NA2···GA1	2.413(1)	0.974(1)	1.456(2)	0.047(2)	0.904(2)	0.040	-0.027	0.095
			2.413	0.996	1.431	0.054	0.906	0.047	-0.034	0.005
7	O13···H20—C20	NA2···NA1	2.637(1)	1.566(1)	1.116(1)	0.046(2)	0.692(2)	0.034	-0.020	0.101
			2.637	1.498	1.160	0.042	0.654	0.034	-0.020	0.150
8	C4···C19	GA1···NA1	3.243(1)	1.706(2)	1.581(1)	0.046(2)	0.516(1)	0.027	-0.020	0.706
			3.243	1.668	1.603	0.041	0.493	0.027	-0.020	1.131
9	C6···O1	GA1···GA1	3.207(1)	1.673(1)	1.556(2)	0.042(1)	0.560(1)	0.027	-0.020	1.284
			3.207	1.658	1.564	0.037	0.539	0.027	-0.020	1.131
10	C16···O14	NA1···NA2	3.332(1)	1.713(1)	1.650(1)	0.042(2)	0.485(1)	0.020	-0.013	0.442
			3.332	1.735	1.635	0.035	0.460	0.020	-0.013	0684
11	O4···C24	GA1···NA2	3.195(1)	1.572(1)	1.624(2)	0.041(1)	0.547(2)	0.027	-0.020	0.649
			3.195	1.575	1.622	0.036	0.518	0.027	-0.013	0.862
12	O9···H23—C23	GA2···NA2	2.554(1)	1.559(2)	1.066(1)	0.037(2)	0.654(1)	0.034	-0.020	1.267
			2.554	1.521	1.074	0.045	0.716	0.034	-0.020	0.899
13	C18···O9	NA1···GA2	3.252(1)	1.675(1)	1.591(2)	0.036(3)	0.490(1)	0.020	-0.013	1.077
			3.252	1.671	1.590	0.033	0.470	0.020	0.013	1.499
14	C26···O11	NA2···NA1	3.304(1)	1.682(2)	1.636(1)	0.033(2)	0.410(1)	0.020	-0.013	0.042
			3.304	1.677	1.639	0.028	0.385	0.020	-0.013	0.061
15	O7···O8	GA2···GA2	3.237(1)	1.594(1)	1.652(2)	0.032(3)	0.506(1)	0.020	-0.013	0.238
			3.237	1.600	1.651	0.032	0.501	0.020	-0.013	0.477

16	O15—H15B···O17	O15water···O17water	2.856(1)	1.169(2)	1.701(1)	0.032(3)	0.482(1)	0.027	-0.013	1.417
			2.856	1.150	1.708	0.039	0.535	0.027	-0.013	1.517
17	O16···H24—C24	O16water···NA2	2.598(1)	1.590(1)	1.041(2)	0.032(2)	0.614(1)	0.027	-0.013	0.259
			2.598	1.545	1.075	0.042	0.651	0.034	-0.020	0.208
18	C24—H24···O7[i]	NA2···GA2	2.640(1)	1.090(1)	1.559(1)	0.032(2)	0.551(1)	0.027	-0.013	0.106
			2.640	1.104	1.537	0.042	0.625	0.027	-0.020	0.292
19	C14—H14A···O10	GA2···GA2	2.828(1)	1.240(2)	1.665(1)	0.030(2)	0.450(1)	0.020	-0.013	0.247
			2.828	1.243	1.631	0.034	0.472	0.020	-0.013	0.444
20	C3—H3A···O14	GA1···NA2	3.012(1)	1.408(1)	1.629(2)	0.030(1)	0.402(2)	0.020	-0.013	0.415
			3.012	1.400	1.628	0.029	0.400	0.020	-0.013	0.513
21	C20—H20···O16	NA1···O16water	3.083(1)	1.376(2)	1.748(1)	0.029(3)	0.403(1)	0.020	-0.013	1.417
			3.083	1.346	1.770	0.032	0.421	0.020	-0.013	0.817
22	O6···O10	GA2···GA2	3.228(1)	1.623(1)	1.605(1)	0.028(3)	0.459(1)	0.020	-0.013	0.324
			3.228	1.608	1.623	0.026	0.446	0.020	-0.013	0.137
23	N1···C20	NA1···NA1	3.636(1)	1.793	1.865	0.024(1)	0.315	0.013	-0.007	1.078
			3.636	1.783	1.881	0.023	0.311	0.013	-0.007	0.879
24	O8···C19	GA2···NA1	3.500(1)	1.703(1)	1.856(1)	0.023(3)	0.307(1)	0.013	-0.007	0.410
			3.500	1.680	1.870	0.021	0.309	0.013	-0.007	0.449
25	C23—H23···O17	NA2···O17water	3.068(1)	1.444(1)	1.688(1)	0.017(1)	0.267(1)	0.007	-0.007	0.756
			3.068	1.397	1.686	0.020	0.294	0.013	-0.007	0.302
26	H10A···H25	GA2···NA2	2.249(1)	1.130(1)	1.162(1)	0.014(1)	0.390(2)	0.013	-0.007	0.079
			2.249	1.113	1.141	0.029	0.458	0.020	-0.013	0.011
27	H17···H18	NA1···NA1	2.898(1)	1.467(1)	1.475(1)	0.012(2)	0.171(1)	0.007	-0.005	0.303
			2.898	1.449	1.462	0.014	0.194	0.007	-0.047	0374
28	C7—H7A···O14	GA1···NA2	3.465(1)	1.526(1)	2.023(1)	0.004(2)	0.072(1)	0.003	-0.001	0.904
			3.465	1.546	1.928	0.005	0.084	0.003	-0.002	0.001

Symmetry codes: (i) *x*-1, *y*, *z*-1; (ii) *x*-1, *y*+1, *z*; (iii) *x*, *y*-1, *z*-1; (iv) -*x*, -*y*+1, -*z*+1; (v) *x*+1, *y*-1, *z*; (vi) *x*+1, *y*, *z*+1; (vii) -*x*+1, -*y*+1, -*z*+1; (viii) -*x*+1, -*y*+1, -*z*+2; (ix) -*x*+2, -*y*+1, -*z*+2; (x) *x*, *y*+1, *z*+1.

Table S5: Ellipticity (ε) of intermolecular H bonds. The upper line in each pair gives the experimental values and the lower one the theoretical values; the statistical errors are estimated based on ref 66.

	Interactions	Interacting species	ε
1	O14···H14—N1	NA2 ···NA1	0.001
			0.003
2	N2—H2···O11[i]	NA2 ···NA1	0.010
			0.006
3	O15···H1—O1	O15water···GA1	0.046
			0.005
4	O12···H8—O8	NA1···GA2	0.122
			0.007
5	O2···H10—O10	GA1···GA2	0.066
			0.016
6	O16···H3—O3	O16water···GA1	0.002
			0.002
7	O7—H7···O16[vi]	GA2···O16water	0.029
			0.014
8	O4—H4···O17	GA1···O17water	0.077
			0.003
9	O16—H16A···O17[iv]	O16water···O17 water	0.044
			0.010
10	O16—H16B···O13[vii]	O16water···NA2	0.173
			0.006
11	O13···H9—O9	NA2···GA2	0.162
			0.006
12	O15—H15A···O11[ix]	O15water···NA1	0.016
			0.032
13	O17—H17A···O10	O17water···GA2	0.163
			0.006
14	O3···O17	GA1···O17water	0.149
			0.457
15	O6···H15B—O15	GA2···O15water	0.129
			0.059
16	O8···H20—C20	GA2···NA1	0.307
			0.269
17	O5—H5···O11[ii]	GA1···NA1	0.213

			0.016
18		NA1···GA1	0.057
	C17—H17···O4^{v}		0.038
19		O17water···GA2	0.181
	O17—H17B…O6^{i}		0.048
20		NA1···O15water	0.015
	C18—H18···O15^{iii}		0.004
21		NA2···NA1	0.016
	C25—H25···O12^{i}		0.026
22		O15water···GA2	0.099
	O15—H15B···O10		0.028

Symmetry codes: (i) *x*-1, *y*, *z*-1; (ii) *x*-1, *y*+1, *z*; (iii) *x*, *y*-1, *z*-1; (iv) -*x*, -*y*+1, -*z*+1; (v) *x*+1, *y*-1, *z*; (vi) *x*+1, *y*, *z*+1; (vii) -*x*+1, -*y*+1, -*z*+1; (viii) -*x*+1, -*y*+1, -*z*+2; (ix) -*x*+2, -*y*+1, -*z*+2; (x) *x*, *y*+1, *z*+1.

Bond ellipticity index

The bond ellipticity [$\varepsilon = \lambda_1/\lambda_2 - 1$] is an index of the measure of cylindricity of the charge distribution and charge delocalization of an interaction[74]. In the present study, the experimental ellipticity values of N─H···O hydrogen bonds range from 0.001 to 0.010 which indicate their cylindrical nature and localization of the charge. Similarly, for most of the O─H···O interactions the values are close to zero except for O8—H8···O12 and O5—H5···O11^{ii}, being 0.122 and 0.213 respectively which indicate their non-cylindrical nature and delocalization of charge. These two hydrogen bonds are non-linear with their ∠D-H-A being 166.87° and 129.47° respectively. These two bonds also possess lower electrostatic energy-28(3) kJ/mol (Table 3), which shows weak nature of these interactions. For the C─H···O interactions, the ellipticity, is quite higher than previously mentioned strong interactions, ranging from 0.015 to 0.307 which shows that these interactions have an elliptical shape and are stretched. It can be concluded that ellipticity is not only measures cylindricity of a bond, but it is also an index of bond strength. Hydrogen bonds with ellipticity values close to zero possess the highest electrostatic interaction energies (Table 3) while those with higher ellipticity values possess lower electrostatic energies. Bond ellipticity is therefore can be a direct measure of the strength of an interaction. However, the precision and accuracy in the calculation of ellipticity for H bonds, especially for experimental data, is generally not considered reliable. One therefore remains cautious in believing ellipticity indices for H bonds.